Immersive 3-D Teleoperation of a Search and Rescue Robot Using a Head-Mounted Display*

Henrique Martins   Rodrigo Ventura

Institute for Systems and Robotics
Instituto Superior Técnico
Lisbon, Portugal
{hmartins,rodrigo.ventura}@isr.ist.utl.pt

Abstract

This paper proposes an alternative approach to common teleoperation methods found in search and rescue (SAR) robots. Using a head mounted display (HMD) the operator is capable of perceiving rectified images of the robot world in 3-D, as transmitted by a pair of stereo cameras onboard the robot. The HMD is also equipped with an integrated head-tracker, which permits controlling the robot motion in such a way that the cameras follow the operator's head movements, thus providing an immersive sensation to him. We claim that this approach is a more intuitive and less error prone teleoperation of the robot. The proposed system was evaluated by a group of subjects, and the results suggest that it may yield significant benefits to the effectiveness of the SAR mission. In particular, the user's depth perception and situational awareness improved significantly when using the HMD, and their performance during a simulated SAR operation was also enhanced, both in terms of operation time and on successful identification of objects of interest.

1. Introduction

Search and Rescue (SAR) is an important application for mobile robots and it has been the object of extensive studies and increasing research. It is fundamental to act rapidly when possible survivors might be trapped amongst the debris, but in a disaster scenario the conditions are usually too dangerous and/or inaccessible for rescue teams to perform a quick evaluation of the calamity site and perform the rescue operation under safe conditions. The usage of SAR robots permits evaluating the danger area in a shorter amount of time, being of great value to any search and rescue operation [15, 9, 10].

For an efficient teleoperation it is paramount for the operator to have the best situation awareness possible. This is particularly difficult in the cases where the operator does not have direct view of the environment surrounding the robot, as it often happens in SAR operation. Moreover, time is an important variable in this case, as lives can be at stake.

Usually, the captured images by SAR robots are presented in a remote computer graphical user interface (GUI) in between a large number of other information, thus obliging the operator to share his/her attention between the small resolution images and the rest of the interface. In addition, due to space restrictions these images have to be displayed in small scale. Altogether, these issues leave the operator prone to general disorientation and cognitive mistakes, which seriously affects overall performance during the SAR mission [17].

In this paper a solution to address this problem is presented, using a head mounted display (HMD) equipped with an internal head-tracker. This solution enables the user to visualize the incoming video stream in three dimensions (3-D), and also resolves the possible existence of image misalignment (due to lack of robustness of the cameras physical support) using a rectification algorithm. Furthermore, the remote operator has the possibility of controlling part of the robot motion through head motion. This innovative approach deeply improves the user situational awareness and provides him a more intuitive control over the robot operation.

The SAR robot targeted for the presented research is called RAPOSA [12]. It is composed of a main body, an articulated frontal body, and uses two-side track wheels for locomotion. RAPOSA is also equipped with a large number of sensors and actuators, namely two frontal video cameras and a back camera. The original operator interface of RAPOSA is similar to most teleoperated robot interfaces: a GUI displayed in a computer screen, together with an input device (usually one or more joysticks).

The paper organization is the following: after an overview of related work in Section 2, a description of the system architecture is provided in Section 3. Section 4 presents a detailed explanation of the developed *3-D vision module*, which allows the possibility of visualizing RAPOSA's captured images in the HMD, instead

of using the existing GUI. Section 5 describes the *head-teleoperation module* and how the head teleoperation of RAPOSA is achieved. The usage evaluation results are described in Section 6. Finally, Section 7 closes the paper with conclusions drawn and a discussion of potential future work.

2. Related Work

The usage of head-mounted devices [4] has been rapidly increasing in distinct areas, such as computer-aided surgery (CAS), video gaming, aviation [14], or robotic applications [5]. Depending on the type of application, HMDs may be used for different purposes, whether to simply project an enlarged image on the visor, to superimpose a computer-generated image (CGI) upon a real-world view (*i.e.,* augmented reality), or even to enable the user to interact with the virtual environment, in case it is equipped with a head tracking system. Nonetheless, nowadays, and despite the increasing research related to robotic applications and HMDs, it is still uncommon to find in the literature examples of SAR robotics applications that use the full potentialities that a HMD may offer.

Notwithstanding, one of the best examples of how a HMD may be used to control a SAR robot is presented by L. Zalud *et al.* [19, 22, 20]: *Orpheus* [21] is a mobile robot controlled with a joystick and a HMD with an inertial head-tracker, through a user interface named *ARGOS*. The authors developed a system which allows the possibility of superimposing distinct types of information on the HMD images, such as thermal information, 3-D proximity, amidst other useful types of information. The tracking of the HMD movement is only used to move a blue cross sign on screen display, unlike the solution presented here, where the tracking data is used to move the robot and to compensate for head rotation.

3. System Architecture

The original system architecture consisted of the SAR robot RAPOSA and a remote operation computer, where all the sensory data is shown in a GUI, and through which the human operator controls the robot using a common gamepad. The communication between the robot and the remote console is made via a wireless connection.

The developed work introduces two new modules to the existing architecture of the system, illustrated in Fig.1. The HMD device is connected to the remote console and receives the visual information captured by both frontal stereo cameras via a VGA connection. The HMD has a separate video source for each of its two screens, which makes it possible to feed different visual information to each screen. This is a fundamental requirement to enable the possibility of displaying the robot world in three dimensions (3-D) in the HMD after some image processing, which is performed by the *3-D vision module*.

Furthermore, integrated into the HMD is a three degrees of freedom (3-DOF) head-tracker, which detects the operator's head motion (yaw, pitch, and roll angles) and sends this data to the remote computer. This data is then processed in three different controllers (one for each angle), whose objective is to calculate the control variables to be sent back to the robot's motors, thus making it possible to teleoperate RAPOSA through head motion. This is performed by the *head-teleoperation module*.
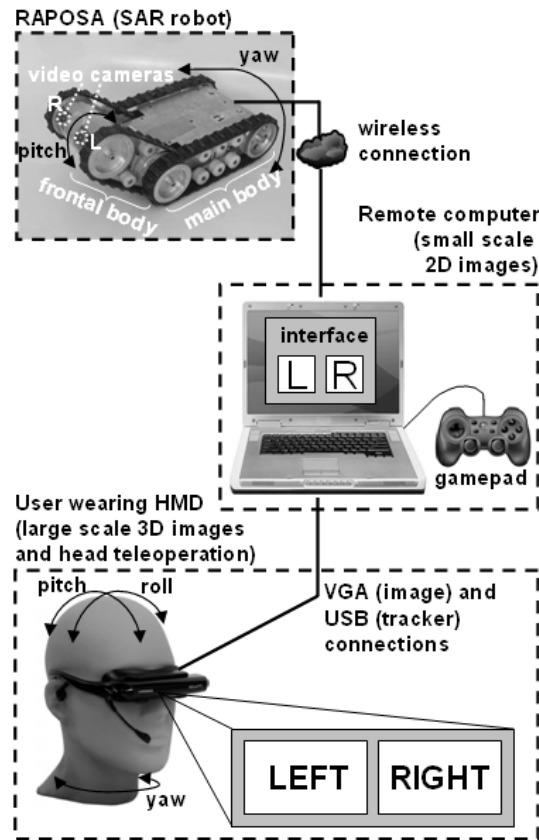

Figure 1. System diagram.

4   3-D Vision Module

The *3-D vision module* aims at providing stereopsis to the human operator, most commonly known as depth perception, by using a HMD. Stereopsis is the process in visual perception leading to the sensation of depth from two slightly different projections of the world onto our eyes, *i.e.,* the capability that any human has of perceiving the world in three dimensions (3-D). Given that the robot has two stereo cameras, it is possible to provide 3-D sensation, starting from the captured pair of 2-D images (hereafter named stereo pair), processing it, and feeding the final result to a device capable of achieving a stereoscopic effect, namely the HMD.

However, the cameras in the robot's frontal body are prone to misalignment, due to mechanical vibration. Displaying the raw images in the HMD as they are captured would cause confusion and eye strain [13]. For this rea-

son, the images are rectified using image processing techniques, prior to displaying them in the HMD. Moreover, they are displayed in the HMD in full screen size, which allows for an improved detail perception.

4.1 Endowing a stereoscopic effect into the images

Firstly, it is necessary to deal with the problem of the images misalignment. This is easily achieved by performing a rotation transformation, so that each image becomes aligned horizontally with the world (e.g., to make world horizon lines become parallel), followed by a crop on the top/bottom sides of each image (hereafter named vertical crop), e.g., world horizon lines become collinear.

One must also take into account the stereo effect delivered by the captured images when visualized on the HMD. This 3-D effect is directly related to the stereo base of the cameras, *i.e.,* the distance separating the left and right cameras, as well as the cameras setup: parallel, converging, or diverging. If the stereo base is too small, the user will perceive the objects of interest with small depth sensation (*cardboard effect*), but if it is too large, it will provoke confusion and *diplopia*, *i.e.,* double vision. Take into consideration that the average male IPD is about $6.3cm$, while RAPOSA's cameras stereo base approximately doubles that value ($11.3cm$). Under these circumstances, if no image processing is performed, the operator would suffer from diplopia. In the literature related to stereographic imagery (stereography) it is possible to find several techniques to adjust the depth in the images suitable for individual user preferences, according to the desired minimum distance of focus[1] [11, 18]. The method chosen is the disparity reduction by left/right shift of the stereo pair images, *i.e.,* an image horizontal crop. This simulates the reduction of the stereo base, and also deals with the inherent problems of the camera setup.

The default horizontal disparity was initially estimated, so that a person with an average IPD could visualize objects in the robot's world at a minimum distance of $1.8m$ with the most comfortable stereo effect possible. However, given that each person's stereo perception varies according to several factors, such as the IPD, or the eye muscles strength [6], this value may be adjusted by the operator until achieving the best stereo effect possible.

4.2 Image rectification algorithm

The proposed rectification algorithm corrects the images misalignment and endows them with a comfortable 3-D effect, by processing a rotation transformation and a crop transformation (vertical and horizontal) on the original stereo pair of images. This adopted solution involves the usage of a common chessboard calibration pattern [1], whose rows must be parallel to the ground (see Fig. 2(a)).

First, the pixel position of all chessboard inner corners is determined using OpenCV's[2]

---

[1]http://nzphoto.tripod.com/stereo/3dtake/ Di_Marzio_Equation_Technical_Web.pdf

[2]http://opencv.sourceforge.net

cvCalibFilter() [2] (as shown in Fig. 2(b)). Given an image I, only the leftmost and rightmost inner corners are considered; for each row k, these corners are denoted (x_a^k, y_a^k) and (x_b^k, y_b^k). The rotation of these rows, relative to the image, is estimated by averaging the angles of the lines formed by these pairs of points, *i.e.,*

$$A(I) = \frac{1}{N} \sum_{i=1}^{N} \arctan\left(\frac{y_b^k - y_a^k}{x_b^k - x_a^k}\right). \qquad (1)$$

Let $A_L = A(I_L)$ and $A_R = A(I_R)$ be the final rotation angles of the left and right images. After calculating A_L and A_R and rotating the images (as shown in Fig. 2(c)), it is necessary to align them vertically and translate them according to the desired eye vergence offset. These alignments can be easily achieved by cropping the images in the opposite borders. For instance, eliminating the topmost Δy pixels from the left image and the bottom Δy pixels from the right image, the two resulting images are moved $2\Delta y$ pixels relative to each other, and *mutatis mutandis* for the horizontal case.

Therefore, it is necessary to recalculate the position of the pattern inner corners of the new rotated images. Consequently, let (x_L, y_L) be one arbitrary inner corner in the left rotated image, and (x_R, y_R) the corresponding corner in the right rotated image, as shown in Fig. 2(c). The crop parameters are obtained in the following way,

$$\begin{cases} \Delta y = y_L - y_R \\ \Delta x = x_L - x_R - D \end{cases} \qquad (2)$$

where Δy and Δx are the amount of pixels to crop vertically and horizontally, and D is the default horizontal disparity chosen. A positive Δx means removing the leftmost Δx pixels of the left image and the rightmost Δx pixels of the right image, and a positive Δy means removing the topmost Δy pixels of the left image and the bottommost Δy pixels of the right image.

Fig. 2(d) shows the resulting images after the whole calibration process. The user may perform a calibration whenever he/she feels necessary. To do so, it suffices to run the calibration algorithm after presenting the chessboard pattern to the robot in the appropriate position. The last calibration data is saved internally and loaded by RAPOSA in each start-up.

During operation, both left and right camera images are subject to the rectification algorithm: a rotation according to (1), followed by a crop according to (2). Both operations are performed by efficient OpenCV routines, thus introducing a negligible computational burden to the operator PC.

5 Head-Teleoperation Module

The HMD has a 3-DOF tracker integrated in it, which permits the detection of the user's head motion, in terms of yaw, pitch, and roll angles. On the other side, the
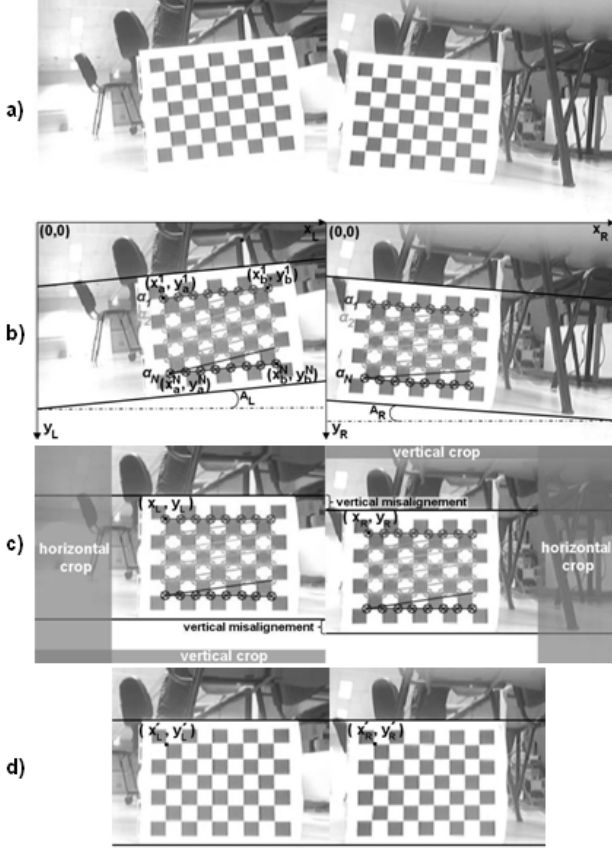
Figure 2. Image rectification algorithm applied to a sample image containing the calibration pattern: a) original unrectified stereo pair; b) detection of the chessboard inner corners; c) stereo pair after rotation transformation; d) stereo pair after cropping transformation

SAR robot can perform yaw movements (by sending symmetric velocities to each of its track wheels) and pitch movements (by ascending/lowering its articulated frontal body), but it is unable to perform roll movements. Hence, the yaw and pitch head angles are used to move the robot, while the head roll angle is used to rotate the image, so that compensating for the head rotation.

5.1 Yaw Controller

The objective of the yaw controller $C_\psi(e_\psi)$ is to control the yaw rotation of the robot, in order to minimize the yaw angle error, *i.e.,* the difference between the yaw angle read by the HMD tracker ψ^{HMD} and the same angle given by the robot's odometry ψ^{ROB}. The nonlinear control law used to compute the robot's angular velocity ω_ψ^{ROB}, given the angular error $e_\psi = \psi^{HMD} - \psi^{ROB}$, is given by

$$\omega_\psi^{ROB} = C_\psi(e_\psi)e_\psi. \qquad (3)$$

The gain $C_\psi(e_\psi)$ depends on the angle error, according to the profile shown in Fig. 3. This gain is zero for a dead zone around zero, in order to make it stop when it is considered to be close enough to the desired goal (besides filtering out sensor noise), constant for high error values, and with a linear profile for smoothness otherwise.
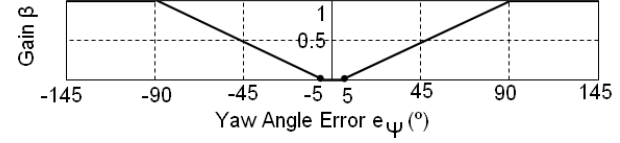

Figure 3. Gain C_ψ as a function of the yaw angle error.

The desired angular velocity is then multiplied by a conversion factor k, in order to convert it into velocities u_l^{ROB} and u_r^{ROB} that will be sent to RAPOSA's left and right track wheels. These velocities are symmetric, so that the robot rotates over itself.

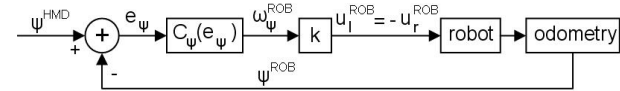In summary, the yaw controller is shown in the blocks diagram of Fig. 4.

Figure 4. Yaw controller blocks diagram.

5.2 Pitch Controller

Similarly to the yaw controller, the objective of the pitch controller $C_\theta(e_\theta)$ is to control the robot's frontal body, in order to minimize the pitch angle error e_θ, *i.e.,* the difference between the HMD pitch angle θ^{HMD} and the robot's frontal body pitch angle θ^{ROB}. The frontal body is controlled with a discrete signal u_a^{ROB}, either to maintain the frontal body current position (0), move it up (-1), or move it down (+1). Given an error $e_\theta = \theta^{HMD} - \theta^{ROB}$, the control signal u_a^{ROB} in function of this error is shown in the profile of Fig. 5. The resulting pitch controller diagram is shown in Fig. 6.
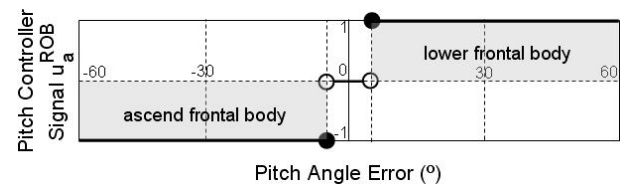

Figure 5. Pitch controller signal as a function of the pitch angle error.

5.3 Roll Movement

When we roll our head, the images projected in our retina rotate accordingly. This does not happen while using a HMD, since it rotates together the head. Hence, in
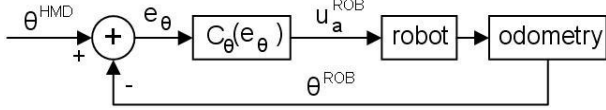
Figure 6. Pitch controller blocks diagram.

order to compensate for this, the displayed images in the HMD are rotated accordingly. The rotation angle is the roll angle measured by the HMD tracker. Fig. 7 shows the resulting transformed images which are seen on the HMD, according to the roll angle as measured by the the HMD tracker.
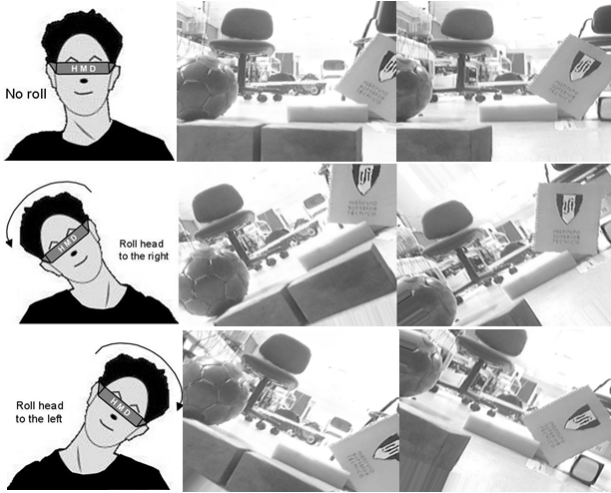

Figure 7. HMD output when rolling head.

6   Usage evaluation

A group of ten subjects were asked to perform several experiments in order to evaluate and compare different aspects of the proposed visualization/control system relatively to the existing system architecture. The following sections describe each experiment and present the corresponding results.

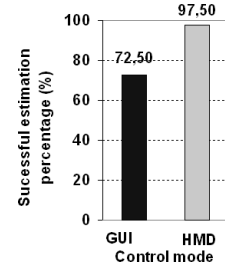### 6.1   Experiment I — Depth perception

The goal of this experiment was to evaluate the users depth perception when visualizing the robot's world using a traditional 2-D GUI and when using the proposed system. A set of objects differing in shape, color, and size, were strategically placed in the scenario, whose top view is shown in Fig. 8. The objects formed areas which incorporated different challenges to the depth perception of the users: in *Area A* the relative distance between the objects is very similar; the objects shape in *Area B* is identical; *Area C* objects equally shaped and coloured, but with different sizes; each object of *Area D* blocks the view of the further object, making it difficult to perceive their shape. The users task consisted in estimating the relative distance between each object, stating which objects are closest to/furthest from the robot. In order to do so, they

were asked to draw two sketches of the scenario's top view according to their perception, both using the GUI and using the HMD. Each of the four areas of both sketches was evaluated with a mark ranging from zero (failure) to three (success), according to how close the sketch is from reality.

The comparative results of the users average score per area , is depicted in Fig. 9(a), where it is possible to observe that the users average performance using the HMD was substantially better in every area comparatively to the GUI . Furthermore, Fig. 9(b) shows the percentage of non-zero scores, across all areas and users, for each interface device (HMD and GUI).
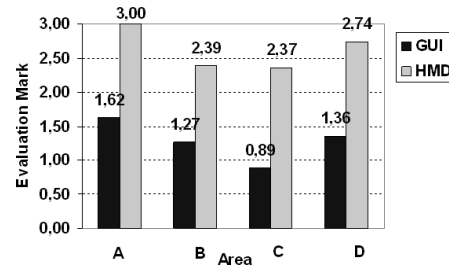
(a) Average score for each area.

(b) Successful estimation per control mode.

Figure 9. Experiment I results.

Hence, these results confirm that the *3-D vision module* successfully provides depth perception to the user.

6.2   Experiment II — Detail perception

This experiment aimed at evaluating whether full screen, large scale images displayed in the HMD offer any advantage over the small scale images of the previous GUI, when it comes to the perception of complex details in a scenario.

Several objects O_i, $i = 1, ..., 6$, with different shapes, sizes and colors are initially shown to the users and then placed in a scenario, either totally visible or partially occluded. The users were then asked to find each object and to evaluate their own perception level, when using the GUI (N_{IIb}^{GUI}) and when using the HMD (N_{IIb}^{HMD}), by attributing a mark ranging from zero (unable to find object) to ten (object detected without any doubt).

Fig. 10(a) shows the average results of this experiment for both interface devices (N_{IIb}^{GUI} and N_{IIb}^{HMD}), as well as the difference between them ($\Delta N_{IIb} = |N_{IIb}^{GUI} - N_{IIb}^{HMD}|$), while Fig 10(b) depicts the percentage of suc-
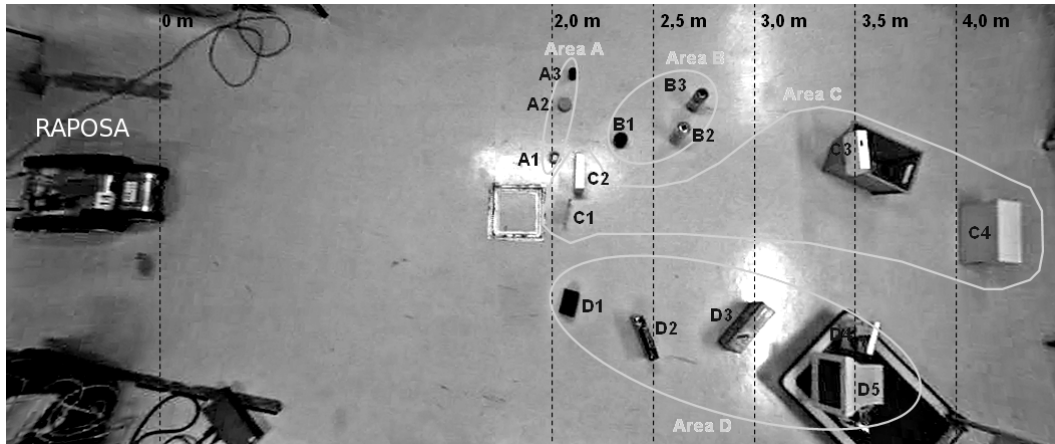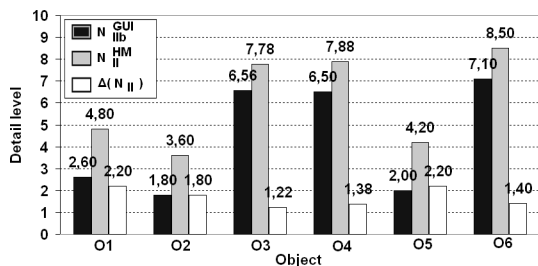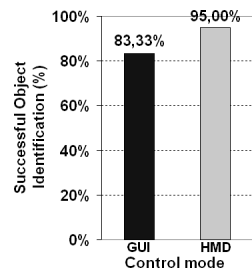
Figure 8. Scenario of Experiment I.

cessful object identifications for both interface devices. From these results, the following conclusions can be drawn:

(a) Average identification performance per object.

(b) Percentage of correct object identifications per interface device.

Figure 10. Experiment II results.

- for each object, the average detail perception level was always better when using the HMD than when using the GUI. On average, the identification performance enhanced approximately 17% when using the HMD;

- the HMD is especially useful in the identification of small objects, namely O_1, O_2 and O_5 (these are the smallest of the test set), with an improvement in the identification performance of 22%, 18% and 22%, respectively;

- the percentage of successful object identification improved approximately 12% when using the HMD

$(95.00\%$ versus 83.33% in Fig. 10(b)).

The obtained results show that, although having the same resolution, the full screen images displayed in the HMD enhance the user perception of small details in a complex scenario, thus improving considerably his situation awareness.

6.3 Experiment III — Execution of a SAR operation

In this experiment, subjects were asked to perform a simple simulated SAR operation, which consisting of: (1) initiating the operation from a fixed starting point, (2) analyzing the scenario, (3) detecting and taking snapshots of possible objects of interest (whose amount is unknown), and (4) returning to the starting point. The performance of each user evaluated, both in terms of the operation time and of the successful identification of objects of interest.

In order to simulate, in the most realistic way, the challenges associated with collapsed structures, the scenario was built taking inspiration from the *Reference Test Arenas for Autonomous Mobile Robots* developed by NIST (*National Institute of Standards and Technology*) [16, 8, 9]. These reference test scenarios for SAR robots, with a total area of about $50m^2$, are divided in three arenas (increasingly more challenging): yellow arena, orange arena and red arena, which provide different challenges to the robots, such as random mazes, stairs, ramps, blocked means of access, and so on. Fig. 11 depicts the scenario built for Experiment III and highlights the several challenges which were incorporated into it, based on the *NIST* reference test arenas.

Each user performed the SAR operation three times, in order to compare the effectiveness of controlling RAPOSA in three different modes:

- M_1 — using solely the GUI;

- M_2 — using the HMD with the *3-D vision module*, and with the yaw, pitch and roll control of the *head-teleoperation module*;
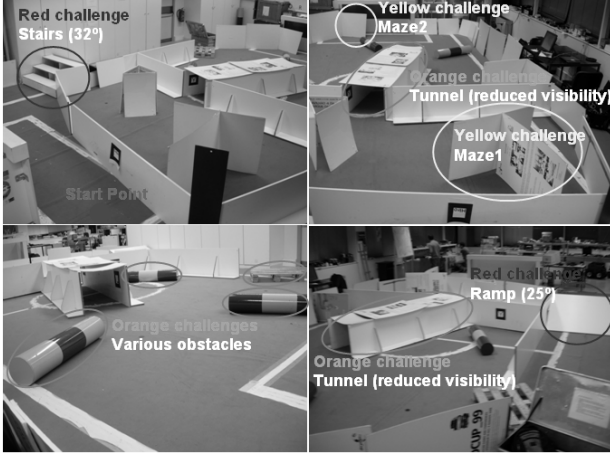
Figure 11. Test arena of Experiment III.

- M_3 — using the HMD with the *3-D vision module*, with the pitch and roll control, but no yaw control.

Fig. 12(a) presents the average operation time T for each control mode M_k, $k = 1, ..., 3$, and Fig. 12(b) shows the percentage of successful object identifications (100% if all objects were identified) per control mode. From these graphics it is possible to observe that:
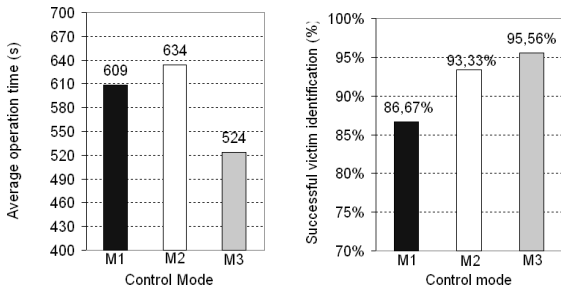
(a) Average operation time per control mode.

(b) Percentage of object identifications per control mode.

Figure 12. Experiment III results.

- the lowest average operation time was obtained for the control mode M_3 (HMD with the yaw controller deactivated). When using this control mode, the users took 14% less time to perform the SAR operation than when using the control mode M_1 (GUI), and enhanced their time performance by 17% comparatively to the control mode M_2 (HMD with all the controllers activated);

- the users time performance is the best when using the HMD without the yaw control, but it is the worst when also using the HMD but with yaw control. The following example explains this counter-intuitive result: when a human being is walking forward and wants to look to the left/right, his natural movement is merely turning the head to the left/right, without altering the forward movement, *i.e.,* without changing the orientation. However, the yaw controller of

the *head-teleoperation module* obliges the robot to change its orientation (robot yaw angle). This causes some confusion to the users, jeopardizing the usability of the robot and, consequently, worsens the operation time to perform the SAR operation;

- the highest percentage of successful object identifications corresponds to the control mode M_3 with $95, 56\%$, followed closely by the control mode M_2 with $93, 33\%$, while the worst performance is related to the control mode M_1 with $86, 67\%$. This result shows that controlling the robot with the HMD increases the effectiveness in the detection of objects of interest, mainly due to the HMD allowing the possibility of displaying the robot world in three-dimensional and in large scale images, compared to the small scale 2-D images of the GUI.

In summary, from the results obtained in Experiment III it is possible to conclude that using the HMD to control the SAR robot RAPOSA, enhances the effectiveness of a SAR operation, on the grounds that it reduces the operation time and improves the successful identification of objects of interest. This is due to the fact that the *3-D vision module* allows the possibility of perceiving the robot world in 3-D and in large scale, thus contributing for a much more immersive experience and greatly improving the situation awareness. It is also related to the fact that the *head-teleoperation module* enhances the usability and controllability of the robot. However, the usage of yaw control worsens this usability, whereby only the pitch and roll controllers should be considered as valid options.

7 Conclusion and Future Work

The proposed visualization/control system of the SAR robot RAPOSA is based on a HMD with an integrated head-tracker, and endowing the operator with the capability of perceiving the robot world in 3-D. The possible vertical and rotational misalignment of the stereo pair of cameras is rectified. Moreover, the operator is capable of controlling part of the robot's motion through head motion.

In order to evaluate the developed modules, a group of subjects were asked to test and compare the existing architecture to the system proposed in this work. The most important conclusions collected from the results:

- compared to the images displayed in the remote console GUI, displaying rectified 3-D large scale images in the HMD, improves the user perception of depth and the estimation of relative distances by 25%, enhances the perception and identification of details in a scenario approximately 17%, and adds to the immersiveness felt by the operator;

- using the HMD to control part of the robot motion improves the usability by reducing the complexity of

operation, especially at an initial stage. The control of the robot becomes more intuitive and less error prone. Notwithstanding, the yaw controller was considered unpractical, given that the robot should not change its orientation according to the HMD yaw motion;

- the users performance during a SAR operation was enhanced when using the HMD. Not only did the operation time reduce about 14%, but the successful identification of objects of interest also improved. This suggests that the HMD improves the effectiveness of a SAR operation.

Future work on this project should focus on incorporating a pan and tilt mounting to the stereo camera pair. This mounting would be controlled independently from the orientation of the robot, and would move according to the HMD motion instead of the robot itself [7], thus enhancing the robot's usability.

Another enhancement which should be addressed in a near future is the intelligent superimposition of key information on the HMD images [22, 20], so that the remote operator is more aware of the robot's sensory data. Notwithstanding, it should be taken into consideration that too much irrelevant information in short periods of time translates into cognitive overload and reduced situational awareness. Hence, only key information should be overlaid on the HMD images (e.g., pop-up messages warning about important events, such as low battery level, dangerous gas readings, and so on). Facilitating this type of information on the HMD images could potentially be an important breakthrough to the effective human-robot interaction, and a major advancement to possibly reducing the current minimum 2:1 human-to-robot ratio [3].

References

[1] S. Arca, E. Casiraghi, and G. Lombardi. Corner localization in chessboards for camera calibration. In *Proceedings of International Conference on Multimedia, Image Processing and Computer Vision (IADAT-micv2005)*, 2005.

[2] M. Bleyer and M. Gelautz. Video-based 3d reconstruction of moving scenes using multiple stationary cameras. In *27th Workshop of the AAPR*, pages 181–187, 2003.

[3] J. Burke and R. Murphy. Human-robot interaction in usar technical search: two heads are better than one. *13th IEEE International Workshop on Robot and Human Interactive Communication (ROMAN-2004).*, pages 307–312, Sept. 2004.

[4] O. Cakmakci and J. Rolland. Head-worn displays: A review. *Journal of Display Technology*, 2(3):199–216, 2006.

[5] M. Fiala. Pano-presence for teleoperation. In *Proceedings of Intelligent Robots and Systems (IROS)*, pages 3798–3802, 2005.

[6] L. Hill and A. Jacobs. 3-d liquid crystal displays and their applications. *Proceedings of the IEEE*, 94(3):575–590, March 2006.

[7] S. Hughes, J. Manojlovich, M. Lewis, and J. Gennari. Camera control and decoupled motion for teleoperation. In *In proceedings of the 2003 IEEE International Conference on Systems, Man, and Cybernetics*, pages 5–8, 2003.

[8] A. Jacoff, E. Messina, and J. Evans. Experiences in deploying test arenas for autonomous mobile robots. In *Proceedings of the 2001 Performance Metrics for Intelligent Systems (PerMIS) Workshop*, 2001.

[9] A. Jacoff, E. Messina, B. A. Weiss, S. Tadokoro, and Y. Nakagawa. Test arenas and performance metrics for urban search and rescue robots. In *Proceedings of the 2003 IEEE/RSJ International Conference on Intelligent Robots and Systems*, 2003.

[10] L. Jinguo, W. Yuechao, L. Bin, and M. Shugen. Current research, key performances and future development of search and rescue robots. *Frontiers of Mechanical Engineering in China*, 2(4):406–416, 2007.

[11] G. R. Jones, D. Lee, N. S. Holliman, and D. Ezra. Controlling perceived depth in stereoscopic images. *Proceedings SPIE Stereoscopic Displays and Virtual Reality Systems VIII*, 4297:42–53, June 2001.

[12] C. Marques, J. Cristovão, P. Alvito, P. Lima, J. Frazão, M. I. Ribeiro, and R. Ventura. A search and rescue robot with tele-operated tether docking system. *Industrial Robot*, 34(4):332–338, 2007.

[13] J. S. McVeigh, M. Siegel, and A. Jordan. Algorithm for automated eye strain reduction in real stereoscopic images and sequences. In *Human Vision and Electronic Imaging*, volume 2657, pages 307–316, February 1996.

[14] S. J. Merhav and S. LifShitz. Adaptive suppression of biodynamic interference in helmet-mounted displays and head teleoperation. *Journal of Guidance, Control, and Dynamics*, 14(6):1173–1180, 1991.

[15] R. Murphy. Human-robot interaction in rescue robotics. *Systems, Man, and Cybernetics, Part C: Applications and Reviews, IEEE Transactions on*, 34(2):138–153, May 2004.

[16] N. I. of Standards and Technology. Statement of requirements for urban search and rescue robot performance standards. Technical report, National Institute of Standards and Technology, 2005.

[17] J. Scholtz, J. Young, H. Yanco, and J. Drury. Evaluation of human-robot interaction awareness in search and rescue. In *Proceedings of the 2004 IEEE International Conference on Robotics and Automation*, pages 2327–2332, 2004.

[18] M. Siegel and S. Nagata. Just enough reality: comfortable 3-d viewing via microstereopsis. *Circuits and Systems for Video Technology, IEEE Transactions on*, 10(3):387–396, Apr 2000.

[19] L. Zalud. ARGOS – system for heterogeneous mobile robot teleoperation. In *Intelligent Robots and Systems, 2006 IEEE/RSJ International Conference on*, pages 211–216, Oct. 2006.

[20] L. Zalud. Augmented reality user interface for reconnaissance robotic missions. In *The 16th IEEE International Symposium on Robot and Human interactive Communication (ROMAN-2007)*, pages 974–979, Aug. 2007.

[21] L. Zalud, L. Kopecny, and F. Burian. Orpheus reconnaissance robots. In *IEEE International Workshop on Safety, Security and Rescue Robotics (SSRR-2008)*, pages 31–34, Oct. 2008.

[22] L. Zalud, L. Kopecny, and T. Neuzil. 3d proximity scanner integration to rescue robotic system. In *ISPRA'05: Proceedings of the 4th WSEAS International Conference on Signal Processing, Robotics and Automation*, 2005.